



HAL
open science

Characterization of unswept and swept quartz crystals for space applications

Jérémie Lefèvre, Sabine Devautour-Vinot, Olivier Cambon, Jean Jacques Boy,
Pierre Guibert, Rémy Chapoulie, Christophe Inguibert, Delphine Picchedda,
Alain Largeteau, Gérard Demazeau, et al.

► **To cite this version:**

Jérémie Lefèvre, Sabine Devautour-Vinot, Olivier Cambon, Jean Jacques Boy, Pierre Guibert, et al..
Characterization of unswept and swept quartz crystals for space applications. *Journal of Applied
Physics*, 2009, 105 (11), pp.113523. 10.1063/1.3141750 . hal-00395272

HAL Id: hal-00395272

<https://hal.science/hal-00395272>

Submitted on 2 Nov 2023

HAL is a multi-disciplinary open access archive for the deposit and dissemination of scientific research documents, whether they are published or not. The documents may come from teaching and research institutions in France or abroad, or from public or private research centers.

L'archive ouverte pluridisciplinaire **HAL**, est destinée au dépôt et à la diffusion de documents scientifiques de niveau recherche, publiés ou non, émanant des établissements d'enseignement et de recherche français ou étrangers, des laboratoires publics ou privés.

Characterization of unswept and swept quartz crystals for space applications

J. Lefèvre,^{1,a)} S. Devautour-Vinot,² O. Cambon,¹ J.-J. Boy,³ P. Guibert,⁴ R. Chapoulie,⁴ C. Inguibert,⁵ D. Picchedda,⁶ A. Largeteau,⁷ G. Demazeau,⁷ and G. Cibiel⁸

¹*Physicochimie des Matériaux Organisés Fonctionnels, Institut Charles Gerhardt, UMR5253 CNRS-UM2-ENSCM-UM1, CC1503, Université Montpellier II, Place Eugène Bataillon, F-34095 Montpellier Cedex, France*

²*Physicochimie des Matériaux Désordonnés et Poreux, Institut Charles Gerhardt, UMR5253 CNRS-UM2-ENSCM-UM1, CC1503, Université Montpellier II, Place Eugène Bataillon, F-34095 Montpellier Cedex, France*

³*Département Temps-Fréquence, Institut FEMTO-ST, 26 chemin de l'Épitaphe, F-25000 Besançon Cedex, France*

⁴*IRAMAT-CRP2A, UMR CNRS 5060, Université Bordeaux III, F-33608 Pessac, France*

⁵*Department of DEST, ONERA-CERT, F-31000 Toulouse, France*

⁶*GEMMA Quartz & Crystal, F-74008 Annecy, France*

⁷*ICMCB, UPR CNRS 9048, F-33608 Pessac Cedex, France*

⁸*Department of Microwave and Time-Frequency, CNES, 18 Avenue Édouard Belin, F-31401 Toulouse Cedex, France*

(Received 6 November 2008; accepted 1 May 2009; published online 9 June 2009)

Unswept and vacuum-swept synthetic quartz crystals were investigated in order to determine the mechanisms responsible for the radiation sensitivity of this material. Results were obtained by means of infrared (IR) spectroscopy, dielectric relaxation spectroscopy (DRS), and thermoluminescence (TL). First, the effect of vacuum sweeping was clearly demonstrated in IR absorption by a significant decrease in the amount of hydroxyl ions and in DRS by the disappearance of the dielectric loss peak arising from the relaxation of alkali ions. Second, it was shown that swept quartz is less sensitive to irradiation than the unswept crystal. A sharp decrease in the TL sensitivity of the electrolyzed material was observed in the energy range corresponding to the recombination of alkaline-electronic defects. DRS results indicated that the dielectric signal is shifted toward a lower energy range for both types of crystals, suggesting that the irradiation greatly facilitates the relaxation of alkaline species by creating low energy hosting sites. However, this shift is drastically less pronounced in the swept quartz because relaxing species are more stable in this material. Third, a correlation was established in TL between trapped charge carriers at point defects in quartz and the frequency variation in quartz oscillators, which is a very promising result for space applications. © 2009 American Institute of Physics. [DOI: [10.1063/1.3141750](https://doi.org/10.1063/1.3141750)]

I. INTRODUCTION

In space systems, quartz crystals are mainly integrated in ultrastable oscillators (USOs) for different applications in telecommunication, navigation, science, or precise positioning.^{1,2} A high stability of these USOs is required over the lifetime of satellites (from a few years up to 20 years) and their specifications should be compatible with severe environmental conditions.

However, radiation effects due to cosmic rays, trapped protons, and electrons in the Van Allen belt, illustrated in Fig. 1, are responsible for a frequency shift for quartz USO embarked on board of spacecraft having a low-Earth orbit, which impair their performance. One of the major programs concerned by this issue is the Doppler satellite tracking system Doppler orbitography and radio positioning integrated in space (DORIS) developed by the Centre National d'Études Spatiales (CNES) for precise orbit determination and ground location with an accuracy of a few centimeters.³ Since 1990,

it is on board of JASON1 and ENVISAT altimetric satellites as well as of remote sensing SPOT series 2, 4, and 5 satellites. It also flew with SPOT3 and TOPEX-POSEIDON. A new DORIS generation has been designed for JASON2 (launched in June 2008) and will be employed for PLEIADES, ALTIKa, CRYOSAT2, HY2, SENTINEL3, etc.

Previous work showed that radiation sensitivity of USO is essentially due to the quartz resonator.⁴⁻⁹ The frequency fluctuations depend on resonator technology (design), quartz crystal quality (impurities, dislocations, etc.), and also the radiation characteristics (dose, flux, and temperature). Norton *et al.*¹⁰ demonstrated that the signature, magnitude, and direction of frequency variations resulting from 123 MeV proton and low level 1.25 MeV gamma (γ) radiation are nearly identical for a given quartz resonator. These results confirmed by Suter,¹¹ and more recently by Cash *et al.*,¹² indicate that the radiation induced frequency changes are primarily ionization effects. Consequently, γ radiation data for low level radiation exposures can be accurately used to predict the performance of a resonator when subjected to proton radiation. This is very convenient because γ irradiation

^{a)}Author to whom correspondence should be addressed. Electronic mail: jeremie.lefevre@polytechnique.edu.

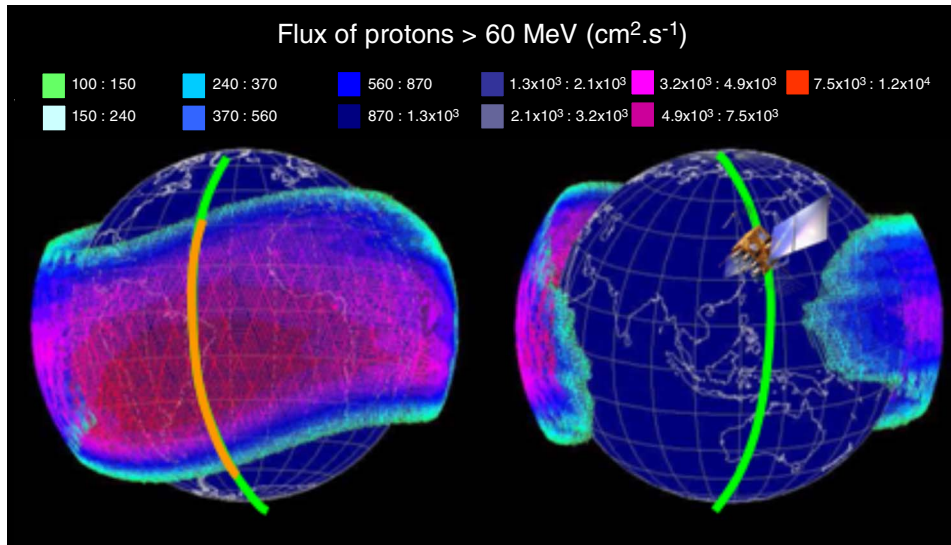


FIG. 1. (Color online) Spatial distribution of solar energetic protons (greater than 60 MeV) (left) in the usual South Atlantic anomaly (SAA) region and (right) at SAA antipodes. Satellites having a polar low-Earth orbit are submitted to periodic irradiations.

tors, contrary to proton accelerators, are relatively inexpensive and offer the possibility of adjusting the radiation dose rate either by using shielding or varying the distance between the device under test and the source. Since electrons (β) in the MeV energy range mainly interact through ionization processes with matter, β accelerators may also be employed.

In order to understand the mechanisms responsible for the radiation sensitivity of quartz, it is necessary to study in detail the material itself. There are numerous tools available to measure the amount of imperfections in crystals and also the displacement or recombination of defects such as inductively coupled plasma (ICP) and glow discharge mass spectrometry for chemical analyses, x-ray topography for dislocations, electron paramagnetic resonance for paramagnetic defects, infrared (IR) spectroscopy for proton content, thermoluminescence (TL) for trapped charge carriers at point defects, and dielectric relaxation spectroscopy (DRS) for charges dynamics. These last three spectroscopic techniques are jointly used within the framework of this study.

The present paper focuses on the fine analysis of unswept and swept synthetic quartz crystals. The first part (Sec. II) describes the studied materials, the sweeping conditions, and then summarizes the experimental procedures. The second part (Sec. III) is dedicated to the characterization by IR, DRS, and TL of quartz samples before and after irradiation and also after a heat treatment at high temperature. The results obtained allow first to select the most appropriate material for space applications in terms of radiation sensitivity and, second, to establish a possible link between microscopic characteristics (population of point defects) and macroscopic properties (mechanical vibrations) of quartz.

II. EXPERIMENTAL DETAILS

The α -quartz crystals investigated in this work were manufactured by the GEMMA Quartz & Crystal Co. They originate from two pure Z-zones of Y-bars with a $16 \times 16 \text{ mm}^2$ square section. The Z faces of one bar were clamped between platinum foil electrodes and swept (electrolyzed) under vacuum at $490 \text{ }^\circ\text{C}$ with an electric field intensity of 2500 V cm^{-1} for about 10 days. Under these con-

ditions, alkali ions located in the vicinity of substitutional aluminum impurities are replaced either by protons released by growth defects to give $[\text{Al}_{\text{Si}}\text{O}_4^-/\text{H}^+]^0(\text{Al}-\text{OH}^-)$ or by electronic holes (h^+) coming from the anode to form $[\text{Al}_{\text{Si}}\text{O}_4^-/h^+]^0(\text{Al}-h^+)$ paramagnetic defects.^{13,14} A comprehensive review of the sweeping phenomenon has been provided by Martin.¹⁵

Samples used for IR experiments were cut in the form of plates ($16 \times 16 \times 5 \text{ mm}^3$) perpendicular to the mechanical Y crystal direction with surfaces optically polished. A NICOLET 750 Fourier spectrometer was used to acquire IR absorption spectra. During measurements, samples were oriented such that the incident light is parallel to the Y axis. Data were obtained at liquid nitrogen temperature (77 K) using a metal Dewar equipped with CaF_2 windows for the IR beam.

Quartz crystals characterized by DRS and TL were SC-cut (defined by $\theta \cong -34^\circ$ and $\phi \cong 22^\circ$ in the IEEE87 Standards) disks of about 9 mm of diameter with a thickness close to 0.5 mm. Dielectric measurements were carried out using a Novocontrol Alpha dielectric analyzer. Blocking electrodes made of $10 \text{ }\mu\text{m}$ thick polytetrafluoroethylene (PTFE) films were inserted between each sample and the metallic electrodes of the apparatus. This allows the dc conductivity contribution of the sample to be transformed into a dielectric loss peak. The temperature dependence of the dielectric loss signal (ϵ'') was measured at fixed frequency ($f = 0.02 \text{ Hz}$) and at a constant heating rate (0.5 deg min^{-1}) for temperatures ranging from -150 to $250 \text{ }^\circ\text{C}$. f was chosen according to the sample conductivity such that the resonant $\epsilon''(T)$ peak is entirely measured in the explored temperature range.

IR and DRS samples were irradiated using a Shepherd irradiator which contains a ^{60}Co (1173 and 1332 keV γ rays) cylindrical sealed source. Irradiation was performed at room temperature (RT) for doses ranging from 10 to 1 kGy with a dose rate of 250 Gy h^{-1} . Quartz crystals characterized by DRS were also submitted to a subsequent annealing treatment at $450 \text{ }^\circ\text{C}$ in air for 24 h.

TL data were recorded by means of an automatic labo-

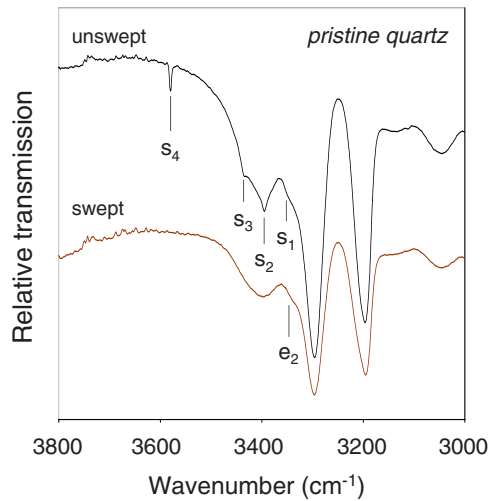


FIG. 2. (Color online) IR spectra obtained at 77 K of an unswept and a vacuum-swept quartz crystal.

ratory designed apparatus¹⁶ composed of a heating finger capable of heating a sample up to 500 °C in a nitrogen atmosphere at a constant rate (2 deg s⁻¹ in this work). The subsequent luminescence was detected by an EMI 9813QKA photomultiplier associated with two Schott BG12 optical filters and one IR rejector. The spectral window was from 350 to 470 nm. A ⁹⁰Sr–⁹⁰Y source delivering electrons (β) at a dose rate of 250 Gy h⁻¹ mounted in our equipment was used to irradiate the samples at RT.

III. RESULTS AND DISCUSSION

A. IR measurements

Figure 2 compares the IR signal of an unswept and a vacuum-swept pristine (unirradiated) crystal. The major feature of both spectra consists of the characteristic relatively broad bands around 3300 and 3200 cm⁻¹, which are associated with the intrinsic Si–O stretching overtone vibrations of the quartz lattice.¹⁷ We also observe a large absorption band in the 3600–3200 cm⁻¹ range superimposed upon several peaks. The nature and the structure of defects correlated with this broad band are not well understood yet. For some authors,¹⁸ it may be related to Si–OH groups and for others,^{19,20} with microbubbles of liquid water (liquid inclusions) or clusters of water molecules such as substitutional (4H)_{Si} defects, in the form of [H₄O₄]⁰ and H₂O interstitial defects.

Only the unswept crystal exhibits the well-known *s* bands located at 3348 cm⁻¹(*s*₁), 3396 cm⁻¹(*s*₂), 3438 cm⁻¹(*s*₃), and 3580 cm⁻¹(*s*₄).²¹ They involve OH groups trapped at impurities during the hydrothermal synthesis of quartz.^{22,21} The electrodiffusion process results in the substitution of the *s*-quadruplet by the *e*₂ band at 3366 cm⁻¹. The latter arises from the presence of protons at Al–O bonds within Al_{Si}O₄ tetrahedra,^{23,24} thus giving [Al_{Si}O₄/H⁺]⁰ defects. It also induces a significant reduction in the intensity of the broad band visible in the 3000 cm⁻¹ region.^{25–28} These observations are consistent with the fact that during the course of vacuum sweeping, Al–OH⁻ defects are formed concomitantly with Al–h⁺ ones^{13,14} due to removal of inter-

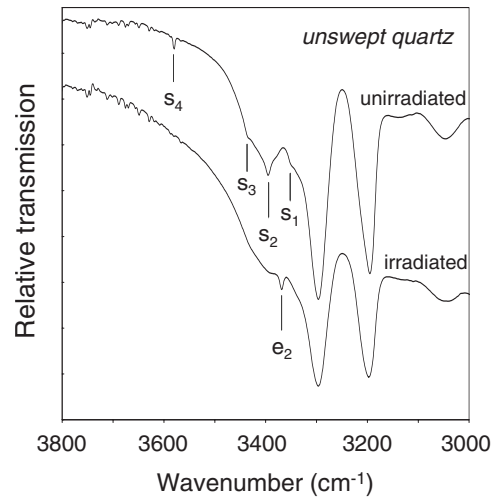


FIG. 3. IR spectra recorded at 77 K of an unswept quartz crystal before and after a 1 Gy γ irradiation dose.

stitial alkali ions from aluminum tetrahedra and their subsequent replacement by protons coming from conventional growth defects.^{24,29–32}

An irradiation at RT of an unswept crystal also induces a drastic reduction in the *s*-quadruplet associated with the appearance of the *e*₂ band (Fig. 3). However, in the present case, the latter is much less intense than that observed in the swept material. In order to understand this observation, one ought to specify that ionizing radiation produces a large number of electron-hole pairs in the insulator materials they pass through. Their presence is especially crucial in quartz because they lead to the radiation-induced mobility of both protons as well as alkali ions above 200 K, thus giving a mixture of Al–h⁺ and Al–OH⁻ defects through mechanisms which are still unclear.^{13,33}

B. DRS measurements

The evolution of the dielectric losses (ϵ'') measured for the unswept and swept pristine quartz materials as a function of temperature is shown in Fig. 4. The increase in the signal

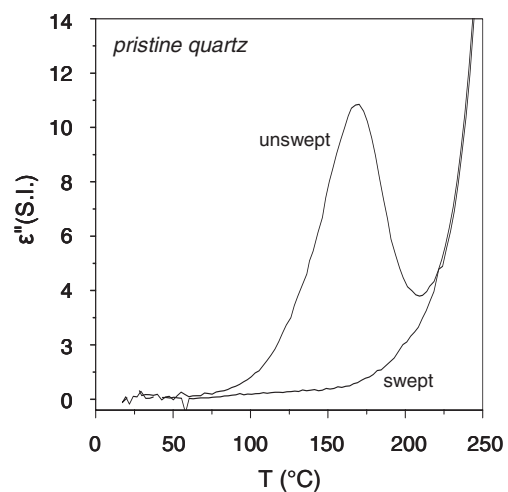


FIG. 4. Dielectric losses (ϵ'') measured at $f=0.02$ Hz vs temperature for an unswept and a vacuum swept quartz crystals.

at high temperature corresponds to the so-called Maxwell–Wagner–Sillars effect which results from the accumulation of ionic charges at the blocking sample-electrode interface. In contrast to the electrolyzed quartz crystal, the unswept sample displays a dielectric loss peak centered at 170 °C. This suggests that the latter material is less stable than the swept one in terms of dielectric properties, which implies that it has charge carriers relaxing at lower energies.³⁴

Dielectric losses arise in quartz from impurities such as alkali ions or protons that possess several crystallographically equivalent orientations with the basic structural unit of the AlSi_3O_4 tetrahedra, among which they may reorient preferentially.³⁵ According to the elementary microscopic process, the potential barrier ΔE to be passed over by charge carriers between two potential minima can be calculated from the relaxation time τ that characterizes the hopping mechanism via the following exponential (Arrhenius) law:

$$\tau = \tau_0 \exp \left[\frac{\Delta E}{kT} \right], \quad (1)$$

where k is Boltzmann's constant, T represents the temperature, and the pre-exponential factor τ_0 is linked to the inverse of the oscillation frequency attributed to the impurity trapped in its host site. We assumed that τ_0 is a constant equal to 10^{-13} s.³⁶ Taking into account that at the peak maximum $\omega\tau=1$, where ω is the electric field pulsations ($\omega=2\pi f$), we then determined the most probable potential barrier (ΔE) to be passed over by the charge carriers. The value of 1.22 eV calculated for the unswept crystal is very close to those obtained for Li^+ and Na^+ implanted quartz materials suggesting that relaxing charge carriers are probably these ion species.³⁷

The detrapping energy of hydrogen ions from aluminum tetrahedra can be expected to be too high to be observed in the explored temperature domain for the chosen fixed frequency f .³⁸ The absence of a dielectric loss peak in the swept material thus agrees with the fact that interstitial alkali ions have been eliminated from the lattice and partially substituted by protons according to IR data.

The evolution of $\epsilon''(T)$ in the case of the unswept and the swept quartz crystals before and after irradiation for doses of 10 Gy, 100 Gy, and 1 kGy is illustrated in Fig. 5. Some signals seem to be poorly resolved probably because of bad contacts between PTFE/metallic electrodes and the sample during measurements. The irradiated unswept crystals display a dielectric loss peak shifted toward low temperatures compared with its position in the pristine state. This tendency is valid whatever the irradiation dose is. We note that the sample exposed to 10 Gy exhibits a peculiar behavior with the appearance of two peaks. Compared to unswept quartz, irradiated swept crystals exhibit a dielectric loss peak with lower intensity and located at higher temperature.

A γ ray exposure with doses of 10 Gy, 100 Gy, and 1 kGy thus induces a decrease in ΔE for both materials. This observation demonstrates that alkali ions are less trapped in the irradiated samples and relax more easily.^{39–42} It is consistent with the fact that upon irradiation at temperatures above 200 K,^{33,43} alkali ions are released from their initial

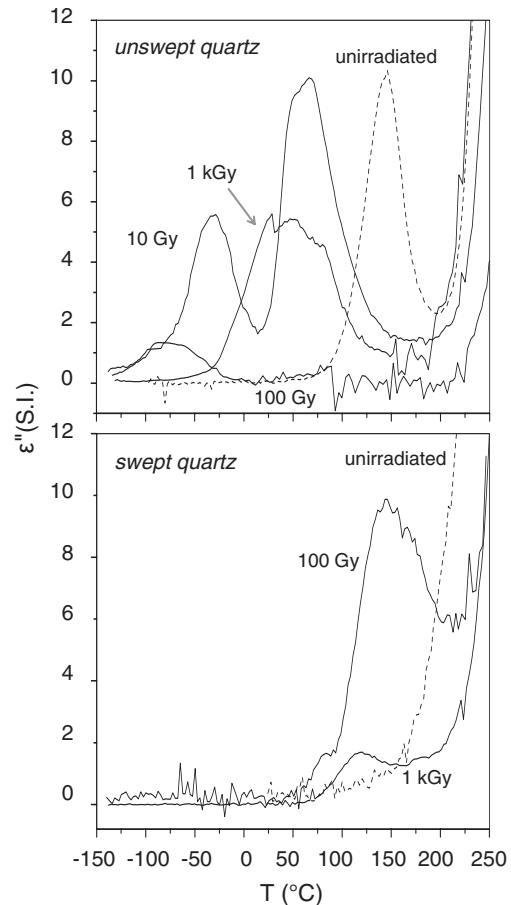


FIG. 5. Dielectric losses recorded at $f=0.02$ Hz vs temperature for unswept and vacuum-swept quartz crystals before (dashed line) and after irradiation (solid line).

host site and replaced by electron holes to form the Al-h^+ defects. The alkali interaction with the oxygen atom of the aluminum tetrahedron thus decreases.

As reported in Table I, the relaxation of charge carriers strongly depends on the irradiation dose in the unswept quartz in contrast to what was already reported for doses greater than 100 Gy.⁴² The following tendency is in quite good agreement with the creation of $[\text{AlSi}_3\text{O}_4/\text{Li}^+]^+$ defects upon irradiation, which was demonstrated by Halliburton *et al.*,⁴⁴

TABLE I. Detrapping energy ($\Delta E \pm 0.02$ eV) obtained from DRS results in the unswept and vacuum-swept quartz materials after 1 Gy, 10 Gy, or 1 kGy γ irradiation and annealing treatment at 450 °C.

		$\Delta E_{\text{unirradiated}}$		
Unswept		1.22		
Vacuum swept		...		
		$\Delta E_{10 \text{ Gy}}$	$\Delta E_{100 \text{ Gy}}$	$\Delta E_{1 \text{ kGy}}$
Unswept		0.66; 0.92	0.54	0.89
Vacuum swept		1.16	...	1.09
		$\Delta E_{10 \text{ Gy}+450 \text{ }^\circ\text{C}}$	$\Delta E_{100 \text{ Gy}+450 \text{ }^\circ\text{C}}$	$\Delta E_{1 \text{ kGy}+450 \text{ }^\circ\text{C}}$
Unswept		1.19	1.18	1.15
Vacuum swept		1.29	...	1.29

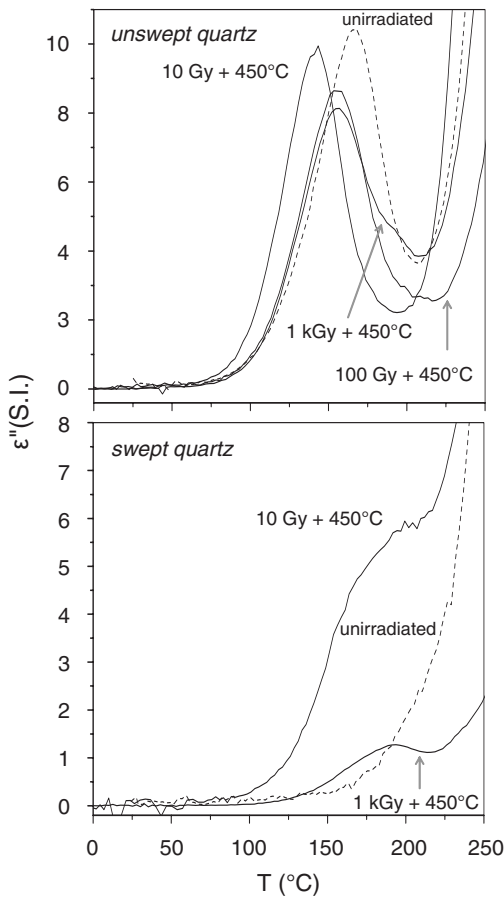


FIG. 6. Dielectric losses recorded at $f=0.02$ Hz vs temperature (above) for unswept and (below) vacuum-swept quartz crystals before irradiation (dashed line) and after an irradiation-plus-annealing treatment at 450°C (solid line).

$$\Delta E_{1\text{ kGy}} < \Delta E_{10\text{ Gy}} < \Delta E_{100\text{ Gy}}.$$

This suggests that the detrapping energy calculated for the irradiated quartz is inversely proportional to the number of lithium-related defects induced by irradiation. The appearance of two dielectric loss peaks in the unswept quartz exposed to 10 Gy may be due to the relaxation of two groups of charge carriers related to Li^+ and Na^+ relaxations, respectively.

In contrast to the untreated quartz, the vacuum-swept material is not very sensitive to the irradiation dose (Table I). This probably results from the high stability of charge carriers in this material. The dielectric loss peak may be linked to H^+ or K^+ ions which were not eliminated during vacuum sweeping.

Dielectric losses of both materials before irradiation and after an irradiation-plus-annealing procedure at 450°C are illustrated in Fig. 6. It is clearly shown that signals of the unswept quartz samples are very similar in position and in shape before irradiation and after annealing. A heat treatment results in a full recovery of the initial $[\text{Al}_{\text{Si}}\text{O}_4^-/M^+]^0$ defects which have been transformed by irradiation, as revealed by ΔE values very close to those obtained for the unirradiated sample. Consequently, the creation of defects by irradiation is perfectly reversible in untreated synthetic quartz upon annealing at 450°C .

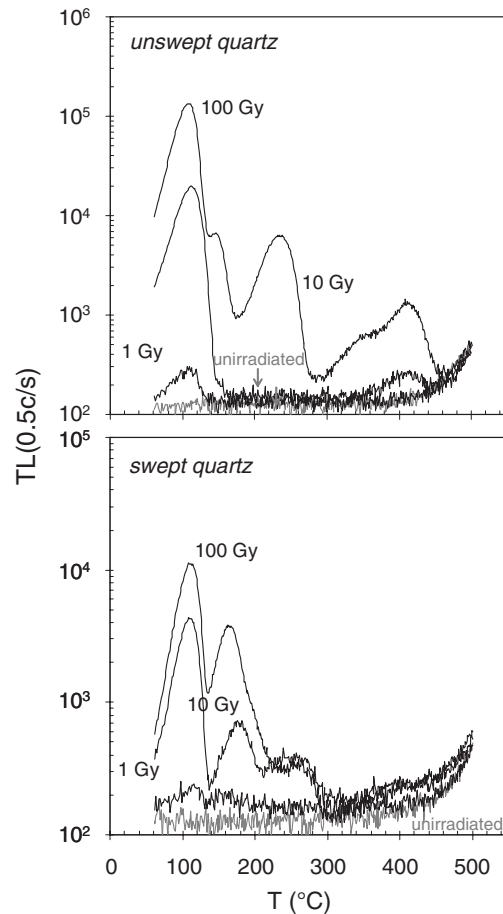


FIG. 7. TL curves taken at a heating rate of 2 deg s^{-1} of unswept and vacuum-swept quartz disks unirradiated and β -irradiated at 1, 10, and 100 Gy.

In contrast, the same annealing conditions are not so optimal in the case of swept crystals because they exhibit a dielectric loss peak centered at 1.29 eV , whereas no peak was observed in the pristine state. This is probably due to the fact that in this material, charge carriers are much too stable to be restabilized in deeper sites upon annealing.

To conclude, it is clearly demonstrated that DRS is a powerful tool for studying the relaxation of alkali ions in quartz crystals. It has been shown that charge carriers in the unswept material (probably Li^+ and Na^+) are less stable than those of the unswept one before irradiation, after irradiation, and also after an irradiation-plus-annealing treatment. From these points of view, the vacuum-swept quartz appears as the most appropriate material for space applications.

C. TL measurements

Figure 7 illustrates the TL response of unswept and vacuum swept quartz crystals before and after 1, 10, and 100 Gy β irradiations. We do not observe any signal in both pristine quartz materials. This behavior is to be distinguished from that of DRS where the local displacement of interstitial alkali ions was observed in the pristine unswept sample. Thus the sole movement of a mobile ion does not give rise to luminescence within the spectral window used ($350\text{--}470\text{ nm}$).

TABLE II. Lifetime (τ in seconds), pre-exponential factor (A), and relative intensity (percent) of four exponential components deduced from TL decay curves after a preheating time at 85 °C.

TL emission peak/domain (°C)	Unswept quartz			Swept quartz		
	τ	A	(%)	τ	A	(%)
110	15	238 300	86.9	15	7000	3.7
130–150	330	9800	3.6
...	680	13 000	69.5
150–200	4800	1100	0.4	5500	50 000	35
200–250	13 500	25 000	9.1

The unswept quartz materials exhibit the well-known peak at 110 °C,^{45,46} the intensity of which increases with the dose. The appearance of numerous TL emissions above 150 °C only after a high irradiation dose (100 Gy) shows a nonlinear growth of the signal in these samples. Concerning the swept crystals, peaks at 110, 170, and 250 °C are detected as well as a weak and broad band above 300 °C. We also observe the disappearance of a shoulder at 140 °C and the appearance of a peak at 170 °C previously observed in a natural quartz.⁴⁷ The intensity of the signals at 110 and 170 °C steadily grows with the dose in contrast to others which saturate above 10 Gy.

After vacuum sweeping, the drastic reduction in the peak at 110 °C and of signals at high temperature can be correlated with the absence of alkali ions in the vicinity of aluminum tetrahedra. Previous works on doped quartz showed that the TL intensity is linked to the concentration of substitutional aluminum (Al^{3+}) associated with an alkali ion as a local charge compensator.^{48,49} In contrast, the presence of H^+ as a compensator for Al^{3+} leads to a decrease in the TL emission. The extrapolation of these conclusions to the pure quartz studied here confirms that the $[\text{Al}_5\text{O}_4^-/M^+]^0$ system is a major source of luminescence in the near UV-blue domain.

Activation energies related to TL peaks (ΔE_{TL}) obtained from the Arrhenius equation in the temperature range from 110 to 250 °C lie between 1.05 (peak at 110 °C) and 1.55 eV (emission at 250 °C) based on measurements performed by Petrov and Bailiff^{50,51} corrected for the thermal quenching of luminescence. These values can be compared with the DRS data of the potential barrier (ΔE_{DRS}) for alkali ions, which are of the same order of magnitude (Table II). We must nonetheless point out that the detrapping energy describing TL mechanisms includes the energy associated with the recombination of an electron-hole pair so that ΔE_{DRS} is necessarily larger than ΔE_{TL} .

The TL process is generally considered to be a result of a transfer of charges (electrons or holes) between an electron trap and a hole trap. Also coupling TL with DRS and IR spectroscopy in quartz clearly demonstrates that this phenomenon is accompanied by a movement of compensator alkali (Li^+ , Na^+ , or K^+) or hydrogen (H^+) ions.

1. Further investigations

Assuming that the frequency shift in USO originates from trapped charge carriers at point defects in the quartz

lattice, we should find common characteristics between the TL properties of the quartz material and the frequency fluctuations of quartz oscillators.

TL decay curves shown in Fig. 8 were recorded for a β -irradiated unswept sample as a function of the preheating time at 85 °C, which is the operating temperature of space USO integrated in the DORIS system. The frame ranging from 110 to 270 °C defines the domain within which a significant decay was observed.

TL components were described in the form of individual exponential decay

$$I_{\text{TL}} = \sum_i A_i \exp\left(-\frac{t}{\tau_i}\right), \quad (2)$$

where I_{TL} is the intensity of the TL peak/emission, A is a pre-exponential factor, t is the decay time (in seconds), and τ represents the lifetime (in seconds) of the i th component. Such an approach is a nontrivial approximation because it corresponds to first-order mechanisms involving uncorrelated trap/centers.

Four main groups of components have been extracted. Their characteristics deduced from an iterative least-squares procedure are given in Table II for the unswept and swept crystals. As reported in Fig. 9, we obtained a linear combination of TL components which reproduces with a good qualitative agreement the frequency variations in an USO

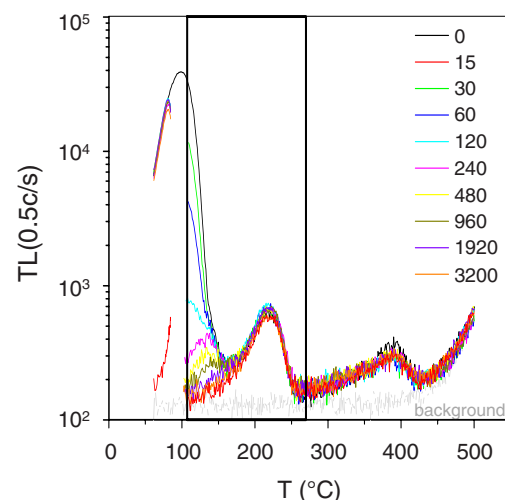


FIG. 8. (Color online) TL decay curves recorded at a heating rate of 2 deg s⁻¹ in an unswept quartz crystal as a function of the preheating time (in seconds) at 85 °C. The frame defines the domain within which a significant decay was observed.

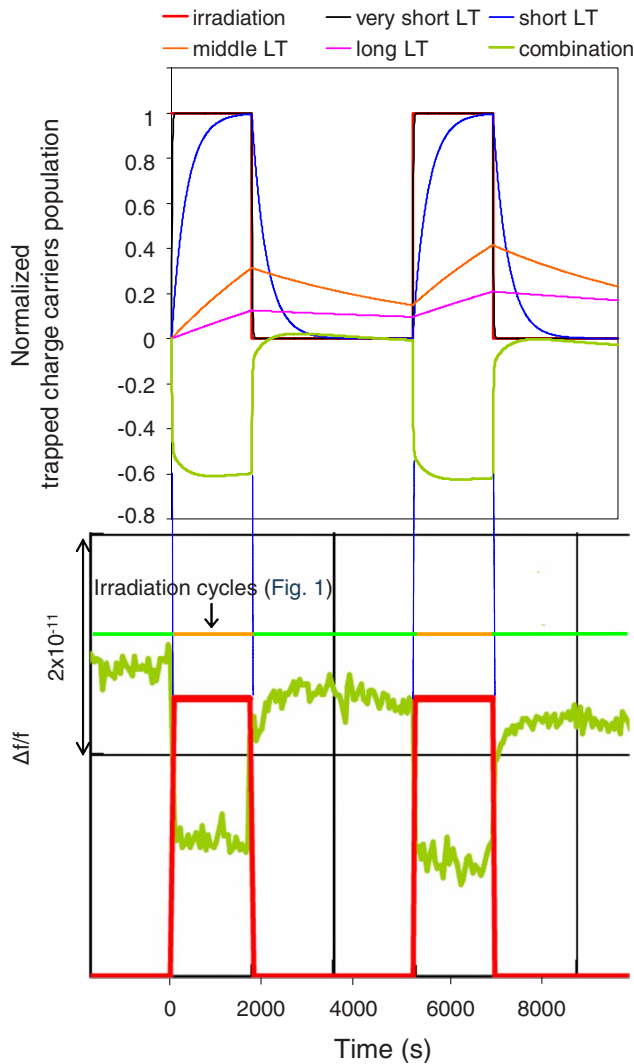


FIG. 9. (Color online) (above) Linear combination of four exponential components given in Table II compared with the (bottom) frequency behavior of a USO using an unswept GEMMA quartz (Ref. 52). This material comes from the batch for the two JASON2 USO.

manufactured with an unswept GEMMA quartz crystal over a 120 min cycle of two 30 min irradiations. This simulates a polar orbital period for space systems at the altitude of the Van Allen radiation belt (Fig. 1). Also to accept this visual correlation, one assumes the following:

- (1) One kind of center (or group of centers) induces a specific sensitivity on the frequency variation.
- (2) The sensitivity to radiation can be negative or positive depending on the nature of the center (the middle lifetime component is negative in our calculations).
- (3) Mechanisms of trapping/relaxation of charge carriers are the same in static conditions (in laboratory) and dynamic conditions (on board of spacecraft).

Calculations indicate that the intermediate (150–200 °C) and long (200–250 °C) lifetime components in contrast to the very short (110 °C) and short (130–150 °C) lifetime ones have a cumulative effect. Indeed, the respective fractions of 50% and 78% of the initial charge carriers are still trapped just before the second irra-

diation. This suggests that the revolution period of 1 h between two irradiations for polar altimetric satellites is not enough such that the crystal relaxes completely. Moreover, keeping in mind that the TL response above 270 °C, which involves very long lifetime components, has not been considered. This could have a significant impact on the long term cumulative frequency shifts.

IV. CONCLUSION

The combined use of different spectroscopic techniques clearly demonstrates, first of all, that the swept quartz is less sensitive to irradiation than the unswept one, as revealed by a sharp decrease in the TL response in the energy domain corresponding to the recombination of alkaline-electronic defects and a less pronounced shift in the dielectric relaxation peak shift toward lower energy of swept crystals in comparison with the untreated ones.

We also reported possible correlations between different methods used to characterize irradiation/thermal effects in quartz. Nevertheless, further investigations are required to perfectly identify the processes responsible for each phenomenon detected in IR, DRS, and TL. This will be possible once the chemical impurities are clearly identified and/or quantified (not only Li and Na but also Ge, Ti, and Fe). Therefore, ICP analysis of the quartz materials investigated in this work is currently in progress.

Finally, by correlating the evolution of the TL properties of quartz with frequency fluctuations of a quartz oscillator, we established a potential link between macroscopic characteristics (mechanical vibrations) and microscopic properties (thermal capture or eviction of trapped charge carriers at point defects) in this material. This is a promising result for space applications. Thus we aim to link the population of charges trapped by irradiation within certain traps with the frequency drift of USO upon irradiation, which is still an open question. This crucial point is actually under study but further investigations are needed to compare the lifetimes of trapped charges with the lifetimes of short and midterm frequency shifts upon and after irradiation.

ACKNOWLEDGMENTS

The authors sincerely thank Dr. J. Détaint and Dr. B. Capelle from the Institut de Minéralogie et de Physique des Milieux Condensés (IMPMC) for fruitful discussions. This work was funded by the CNES, the French space agency.

¹L. E. Halliburton and J. J. Martin, in *Precision Frequency Control*, edited by E. A. Gerber and A. Ballato (Academic, Orlando, 1985), Chap. 1, pp. 1-45.

²B. W. Parkinson and J. J. Spiker, *AIAA J.* **1**, 152 (1996).

³M. Brunet, A. Auriol, P. Agnieray, and F. Nouel, *Frequency Control Symposium*, 49th Proceedings of the 1995 IEEE International, p. 122 (1995).

⁴F. Euler, P. Ligor, A. Kahan, P. Pellegrini, T. M. Flanagan, and T. F. Wrobel, *IEEE Trans. Nucl. Sci.* **NS-25**, 1267 (1978).

⁵P. Pellegrini, F. Euler, A. Kahan, T. M. Flanagan, and T. F. Wrobel, *IEEE Trans. Nucl. Sci.* **25**, 1267 (1978).

⁶T. J. Young, D. R. Koehler, and R. A. Adams, *Proceedings of the 32nd Annual Frequency Control Symposium* (National Technical Information Service, Springfield, VA, 1978), p. 34.

⁷D. R. Koehler and J. J. Martin, *J. Appl. Phys.* **57**, 5205 (1985).

⁸H. G. Lipson, F. Euler, and P. A. Ligor, *Proceedings Annual Frequency*

- Control Symposium 33, US Army Electronics Command, Atlantic City, NJ, 1979, p. 122.
- ⁹F. Euler, P. Ligor, A. Kahan, and P. Pellegrini, in Proceedings of the Annual Frequency Control Symposium, 1978, p. 24.
- ¹⁰J. R. Norton, J. M. Cloeren, and J. J. Suter, in Proceedings of the Thirty-Eighth Annual Frequency Control Symposium, IEEE, New York, 1984, p. 63.
- ¹¹J. J. Suter, *IEEE Trans. Ultrason. Ferroelectr. Freq. Control* **34**, 667 (1987).
- ¹²P. E. Cash, D. A. Emmons, and W. J. Stapor, Frequency Control Symposium, 50th Proceedings of the 1996 IEEE International (1995), p. 10.
- ¹³M. C. M. O'Brien, *Proc. R. Soc. London* **A231**, 404 (1955).
- ¹⁴J. A. Weil, *Radiat. Eff.* **26**, 261 (1975).
- ¹⁵J. J. Martin, *IEEE Trans. Ultrason. Ferroelectr. Freq. Control* **35**, 288 (1988).
- ¹⁶P. Guibert, R. Chapoulie, S. Dubernet, A. Largeteau, and G. Demazeau, Proceedings of TimeNav'07: Joint Meeting of IEEE-IFCS, EFTF and ENC-GNSS, 2007 (unpublished), p. 164.
- ¹⁷H. Bahadur, *J. Appl. Phys.* **66**, 4973 (1989).
- ¹⁸D. T. Griggs and J. D. Blacic, *Science* **147**, 292 (1965).
- ¹⁹R. D. Aines and G. R. Rossman, *J. Geophys. Res., [Solid Earth]* **89**, 4059 (1984).
- ²⁰P. Cordier, J. A. Weil, D. F. Howarth, and J. C. Doukhan, *Eur. J. Mineral.* **6**, 17 (1994).
- ²¹S. H. G. Lipson, F. Euler, and A. F. Armington, in *Proceedings 32nd Annual Frequency Control Symposium IEEE* (1978), p. 11.
- ²²A. Kats, *Philips Res. Rep.* **17**, 133 (1962).
- ²³R. N. Brown and A. Kahan, *J. Phys. Chem. Solids* **36**, 467 (1975).
- ²⁴W. A. Sibley, J. J. Martin, M. C. Wintersgill, and J. D. Brown, *J. Appl. Phys.* **50**, 5449 (1979).
- ²⁵D. M. Dodd and D. B. Fraser, *J. Appl. Phys.* **26**, 673 (1965).
- ²⁶J. J. Boy, B. Boizot, R. Petit, D. Picchedda, and J. P. Romand, Frequency Control Symposium, 2007 Joint with the 21st European Frequency and Time Forum, 2007 (unpublished), p. 199.
- ²⁷J. P. Bachheimer, *J. Phys. IV* **4**, C2-173 (1994).
- ²⁸M. S. Paterson, *Bull. Mineral.* **105**, 20 (1982).
- ²⁹L. E. Halliburton, N. Koumvakalis, M. E. Marques, and J. J. Martin, *J. Appl. Phys.* **4-6**, 513 (1998).
- ³⁰J. J. Martin, *J. Appl. Phys.* **56**, 2536 (1984).
- ³¹G. Lipson and A. Kahan, *IEEE Trans. Nuclear Sci.* **NS-31**, 1223 (1984).
- ³²J. J. Martin, *J. Appl. Phys.* **68**, 5095 (1990).
- ³³M. E. Marques and L. E. Halliburton, *J. Appl. Phys.* **50**, 8172 (1979).
- ³⁴H. Jain and A. S. Nowick, *J. Appl. Phys.* **53**, 477 (1982).
- ³⁵J. Toulouse, S. Ling, and A. S. Nowick, *Phys. Rev. B* **52**, 3122 (1988).
- ³⁶J. Fripiat, J. Chaussidon, and A. Jelli, *Chimie Physique des Phénomènes de Surface* (Masson, Paris, 1971).
- ³⁷C. Poignon, G. Jeandel, and G. Morlot, *J. Appl. Phys.* **80**, 6192 (1996).
- ³⁸A. K. Kronenberg and S. H. Kirby, *Am. Mineral.* **72**, 734 (1987).
- ³⁹A. S. Nowick and H. Jain, in Proceedings of the 34th Annual Frequency Control Symposium, U.S. AERADCOM, Ft. Monmouth, NJ (1980), p. 9.
- ⁴⁰H. Jain and A. S. Nowick, *J. Appl. Phys.* **53**, 485 (1982).
- ⁴¹S. Ling and A. S. Nowick, *Proc. Ann. Symp. Freq. Contr.* **40**, 96 (1986).
- ⁴²S. Devautour-Vinot, O. Cambon, N. Prud'Homme, J. C. Giuntini, J. J. Boy, and G. Cibiel, *J. Appl. Phys.* **102**, 104102 (2007).
- ⁴³K. P. Semenov and A. A. Fotchenkov, *Kristallografiya* **22**, 326 (1977).
- ⁴⁴L. E. Halliburton, C. Y. Chen, and S. D. Tapp, in Proceedings of the 39th Annual Frequency Control Symposium (1985), p. 673.
- ⁴⁵G. Chen and S. H. Li, *J. Phys. D* **33**, 437 (2000).
- ⁴⁶V. Pagonis, G. Kitis, and R. Chen, *Radiat. Meas.* **37**, 267 (2003).
- ⁴⁷H. Y. Göksu, I. K. Bailiff, and V. B. Mikhailik, *Radiat. Meas.* **37**, 323 (2003).
- ⁴⁸P. E. Hickel, G. Demazeau, R. Arnaud, R. Chapoulie, P. Guibert, E. Vartanian, G. Villeneuve, F. Bechtel, and B. Capelle, *High Press. Res.* **18**, 265 (2000).
- ⁴⁹E. Vartanian, P. Guibert, C. Roque, F. Bechtel, and M. Shvoerer, *Radiat. Meas.* **32**, 647 (2000).
- ⁵⁰S. A. Petrov and I. K. Bailiff, *Radiat. Meas.* **24**, 519 (1995).
- ⁵¹S. A. Petrov and I. K. Bailiff, *Radiat. Meas.* **27**, 185 (1997).
- ⁵²G. Cibiel, Frequency Control Symposium, 2007 Joint with the 21st European Frequency and Time Forum, 2007 (unpublished), Vol. 6192, p. 1164.